Sea surface temperature anomalies in the North Pacific Ocean

Richard W. Reynolds

Sea surface temperature anomalies in the North Pacific Ocean

By RICHARD W. REYNOLDS,[1] *Max-Planck-Institut für Meteorologie, 2 Hamburg 13, FRG*

ABSTRACT

Sea surface temperature anomalies in the mid-latitude North Pacific Ocean were compared with a first-order autoregression model in which the anomalies are forced by local atmospheric white noise. The results showed that the model can explain the power spectrum of the anomalies for a little over 50% of the investigated regions, mainly in the central regions of the Pacific, but fails, not surprisingly, in regions of strong oceanographic processes.

1. Introduction

Hasselmann (1976) has proposed a stochastic model of climate variability in which slow changes of climate are explained as the integral response of the climate to continuous random excitation by shorter time-scale disturbances. The entire climate system is divided into two subsystems with widely differing time scales: a rapidly varying "weather" subsystem and a slowly responding "climate" subsystem. The "weather" components are treated as random (white noise) forcing terms. The "climate" components then act as integrators of this excitation. The model predicts that the climate components should exhibit a red power spectrum which for intermediate frequencies is inversely proportional to the frequency squared.

Frankignoul and Hasselmann (1977) have applied the model to a simplified atmospheric and oceanic system. In this system the climatic components were represented as sea surface temperature (SST) anomalies which were driven by uncorrelated white-noise atmospheric forcing. To balance the atmospheric input and maintain a statistically stationary response, a negative stabilizing feedback, characterized by a linear feedback factor, λ, was added where $(2\pi\lambda)^{-1}$ is the e-folding

decay time. With feedback, the SST anomalies have a spectral form, $\hat{E}(f)$, given by:

$$\hat{E}(f) = \frac{A}{f^2 + \lambda^2},\qquad(1)$$

where f is frequency and A is proportional to the variance of the white-noise input spectrum. Equation (1) can be recognized as the spectrum of a first-order autoregression process with random noise.

Frankignoul and Hasselmann (1977) verified (1) by numerical experiments and by comparison with individual weather ship and integrated North Pacific data. In this paper a more detailed regional study of the North Pacific Ocean is presented. Equation (1) is compared with measured SST anomalies for five degree squares to determine in which regions the stochastic climate model is applicable.

2. Procedure

For comparison with real data, (1) must be expressed in terms of the spectrum that would be determined for a discrete time series of sampling interval, Δt. Following Wunsch (1972), (1) becomes:

$$\hat{E}_1(f) = \sum_{m=-\infty}^{\infty} \frac{A}{(f - 2mf_n)^2 + \lambda^2},\qquad(2)$$

---

[1] Present address: Climatic Research Institute, Oregon State University, Corvallis, Oregon, 97331.

where $f_n = 1/(2\Delta t)$ is the Nyquist frequency, m is an integer and $0 \leq f \leq f_n$. The total variance, σ, of (1) and (2) is conserved since:

$$\sigma = \int_0^\infty \hat{E}(f)df = \int_0^{f_n} \hat{E}_1(f)df = \frac{A\pi}{2\lambda}. \qquad (3)$$

With the aid of Cauchy's integral theorem of residues (cf. Copson, 1960, p. 144), (2) can be expressed more simply as:

$$\hat{E}_1(f) = \frac{N_1}{1 + \alpha_1^2 - 2\alpha_1 \cos(\pi f/f_n)}, \qquad (4)$$

where

$$\alpha_1 = \exp(-\pi\lambda/f_n), \qquad (5)$$

and

$$N_1 = A \frac{\pi\alpha \sinh(\pi\lambda/f_n)}{\lambda f_n}. \qquad (6)$$

Equation (3) is the spectrum of a discrete first-order autoregression process which is forced by white noise (cf. Jenkins and Watts, 1968) where α_1 is the autocorrelation of the first lag and N_1 is the variance of the noise.

The measured SST anomalies were obtained from NORPAX data of the mid-latitude (20° N–55° N) North Pacific. The data consisted of $28\frac{1}{2}$ years of monthly average temperatures for a five-degree square grid. To deal with occasional data gaps, each time series was divided into as many subseries of 64 consecutive points as possible. If at least three subseries were obtained for each grid point, the Fourier coefficients for each subseries were computed by a fast Fourier transform. A discrete spectrum, $E(f_j)$, was then calculated from the square of the average of the Fourier coefficients at each frequency. Since the resulting number of spectral degrees of freedom can be shown (Hasselmann, personal communication) to be two times the number of subseries used, $E(f_j)$ had six to maximally ten degrees of freedom. The spectral resolution was 0.19 cycles per year (cpy); the Nyquist frequency was 6 cpy.

To verify the stochastic model for SST anomalies, it must be shown that (4) is an adequate representation of $E(f_j)$ within the statistically prescribed error limits. This was done by determining the two free parameters in (4), α_1 and N_1, at each grid location, by minimizing the deviation, ε,

between E and $\hat{E}$ by a least square fit:

$$\varepsilon = \sum_{j=0}^{p-1} [\ln E(f_j) - \ln \hat{E}(f_j)]^2 = \min, \qquad (7)$$

where the number of spectral points, $p = 33$. A logarithm of the spectrums was used in the definition of ε so that the statistical errors for each spectral frequency would receive equal weight in (7).

A similar least square fit was also made for two extensions of (4), each of which contained three free parameters. The first, $\hat{E}_2(f)$, included an extra noise term, M, such that:

$$\hat{E}_2(f) = \frac{N_2}{1 + \alpha_2^2 - 2\alpha_2 \cos(\pi f/f_n)} + M. \qquad (8)$$

The second, $\hat{E}_3(f)$, represented the spectrum of a second-order autoregression process (Jenkins and Watts, 1968):

$$\hat{E}_3(f) =$$

$$\frac{N_3}{1 + \alpha_3^2 + \beta^2 - 2\alpha_3(1 - \beta)\cos(\pi f/f_n) - 2\beta \cos(2\pi f/f_n)}, \qquad (9)$$

where β is the second-order regression coefficient. In all cases the free parameters (α_1, N_1); (α_2, N_2, M); and (α_3, N_3, β) were determined independently of each other by minimizing ε in (7) for each model spectrum.

To determine which of the model spectrums were statistically significant, the hypothesis was made that the model fits the true spectrum perfectly. However, because of the statistical finite-sampling error, the model spectrum will never fit the measured spectrum exactly, and consequently ε is never zero. The probability distribution of ε is a χ^2-distribution with $p - q$ degrees of freedom where q is the number of fitted parameters in the model spectrum. Since $p - q$ is large the distribution can be approximated as a Gaussian with a mean and variance (see Appendix) given by:

$$\langle \varepsilon \rangle = \frac{2}{\nu}(p - q),$$

$$\sigma_\varepsilon^2 = \langle (\varepsilon - \langle \varepsilon \rangle)^2 \rangle = \frac{8}{\nu^2}(p - q),$$

where ν is the number of spectral degrees of freedom of $E(f_j)$. A critical ε, $\bar{\varepsilon}$, was then defined

such that the probability that $\varepsilon < \bar{\varepsilon}$ is 95%:

$$\bar{\varepsilon} = 1.65\sigma_\varepsilon + \langle\varepsilon\rangle. \tag{10}$$

For each fitted spectrum the model was considered statistically significant, within a 95% confidence limit, if $\varepsilon < \bar{\varepsilon}$.

3. Results

The boxed-in region in Fig. 1 indicates the five-degree squares for which measured spectrums were computed. For each position, ε was determined for
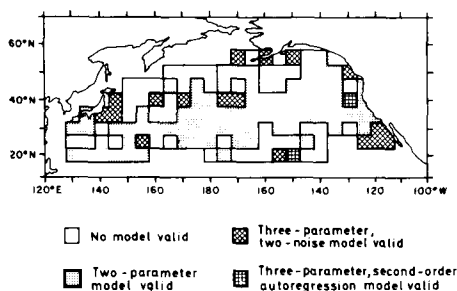

Fig. 1. The regions of validity of the three spectral models (see text).

the two-parameter model (4). The regions in which the fit was significant ($\varepsilon < \bar{\varepsilon}$) are dotted. In the remaining regions, the ε's for both three-parameter models were computed. If both models were significant, the model with the smaller ε was chosen as the "valid" model. An example of the three fitted model spectrums and the measured spectrum is shown in Fig. 2. Here only the two three-parameter models were significant.

The regions in which the two-parameter model is *not* valid (statistically significant) can generally be related to known areas of strong oceanographic processes, such as the Arctic and subtropic convergences. In these regions oceanographic processes are apparently at least as important as the local atmospheric forcing as the cause of SST variability. However, in the remaining "quiet" areas of the ocean (54% of the total), the two-parameter stochastic-forcing model is validated.

The three-parameter models are jointly valid over 20 of the remaining five-degree squares (14% of the total). Although the regions are scattered, they occur principally along the course of the Kuroshio and off the coast of North America. The
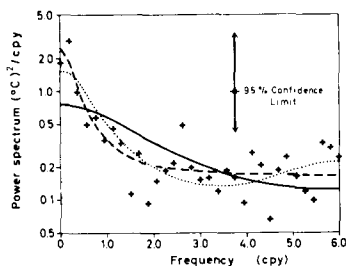

Fig. 2. A sample SST anomaly power spectrum with eight degrees of freedom at 40° N latitude and 145° E longitude. A plus means the measured spectrum, the full line two-parameter model, the dashed line the three-parameter, two-noise model and the dotted line the three-parameter, second-order autoregression model.

three-parameter, two-noise model was generally better (smaller ε) than the second-order auto-regression model. As can be seen in Fig. 1, the second-order autoregression model was found to be better for only two squares (1.4% of the total).

For the valid two-parameter fits of (4), the value of λ was calculated from (5). The mean value, $\bar{\lambda}$, was found to be 1.1 yr^{-1}. In Fig. 3, the regions are shown where λ differed from $\bar{\lambda}$ by more than 15% and more than 30%. It can be seen that the regions of large and small λ can be roughly divided by the 165° W meridian. This may indicate that the Northern Pacific SST anomalies have more thermal inertia in the eastern part.
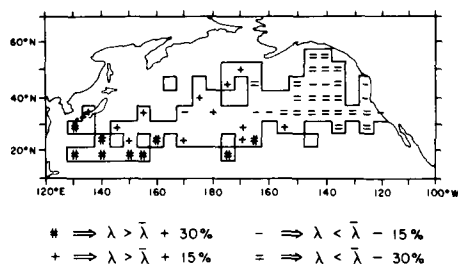

Fig. 3. Regions where the two-parameter model's λ differs from $\bar{\lambda}$ (= 1.1 yr^{-1}). The rectangular lines indicate the boundaries of the valid two-parameter fit from Fig. 1.

The value $\bar{\lambda} = 1.1$ yr^{-1} is larger than the value 0.32 yr^{-1} determined by Frankignoul and Hassel-mann (1977) for the first empirical orthogonal function (EOF) of Davis (1976) for the same data set. The difference may be attributed to the EOF

procedure, which tends to assign the features of shorter wavelengths to higher-order functions. This eliminates much of the short-period noise from the lower orthogonal functions and characteristically lowers the value of λ. To illustrate this effect, the two-parameter model was fitted to the spectrum of the first fifteen EOF. The λ's for statistically valid fits are shown in Fig. 4. As expected the value of λ has increased with increasing EOF order until λ for the tenth EOF is within 10% of $\bar{\lambda}$.
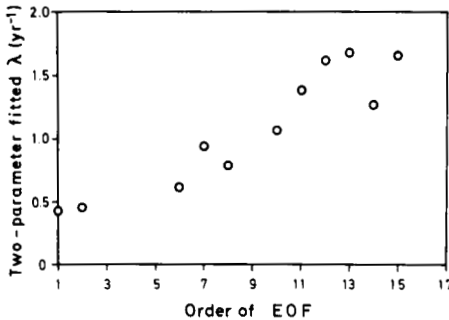

Fig. 4. Values of λ for a statistically valid fit for the empirical orthogonal functions (EOF).

For the valid two-parameter fits, the value of A was determined from (6). In Fig. 5 the regions are indicated in which A differed from the mean, $\bar{A}$, by more than 15% and 30%. Since A is proportional to the white-noise forcing, two regions of strong forcing are indicated. The more important region is at $40°$ N between approximately $170°$ E and $160°$ W.
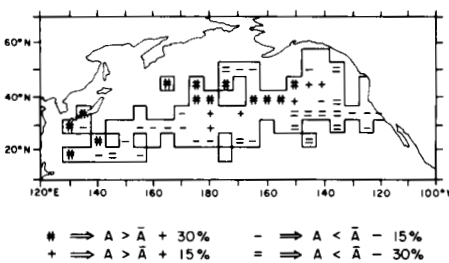

Fig. 5. Regions where the two-parameter model's A differs from $\bar{A}$ (= 0.30 (°C)^2 cpy). See also Fig. 3.

The variance, σ, of the SST anomaly signal which can be attributed to the valid two-parameter fit can now be computed by (3). The distribution of σ is shown in Fig. 6 for regions in which σ differs from the mean value, $\bar{\sigma}$, by more than 15% and
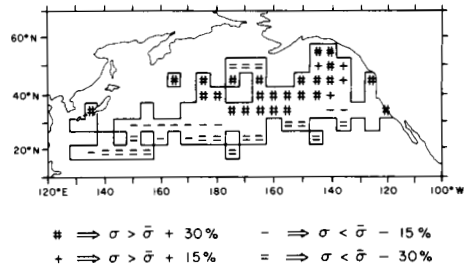

Fig. 6. Regions where the two-parameter model's variance, σ, differs from $\bar{\sigma} = (0.45 \, (°C)^2)$. See also Fig. 3.

30%. For comparison, Fig. 7 shows the distribution of the total SST anomaly variance for the entire region studied. It can be seen that regions of large σ and large total variance are very similar.
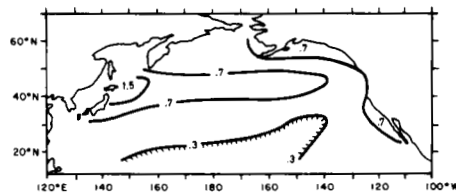

Fig. 7. Distribution of the variance of SST anomalies in (°C)^2. The mean of the variance is 0.58 (°C)^2.

The boundaries of the region of validity of the two-parameter model can also be determined from the sensitivity of the estimates of the model parameters to the least squares fit procedure. For example, an alternate estimate of α can be obtained by least square fitting a first-order autoregression process directly to the original time series of SST anomalies. This yields an α value equal to the first lagged auto-correlation (Jenkins and Watts, 1968); the feedback parameter can then be determined from (5). A relative error, γ, can now be defined as:

$$\gamma = \left| \frac{\lambda - \lambda_{ac}}{\lambda} \right|, \tag{11}$$

where λ is the feedback parameter from the two-parameter model and λ_{ac} is the feedback parameter determined from the auto-correlation. Values of γ were determined for all points irrespective of whether $\varepsilon < \bar{\varepsilon}$ and are shown in Fig. 8. Large values of γ are seen to coincide with the previously defined boundaries limiting the region of validity of the local stochastic forcing model.
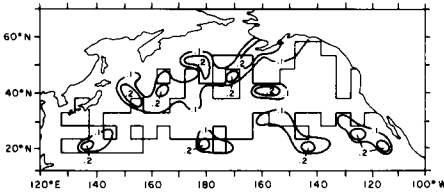
Fig. 8. Distribution of the relative error between the spectral two-parameter fitted λ and the fitted λ_{ac} from the first-lagged autocorrelation. See also Fig. 3.

4. Summary

A little more than 50% of the mid-latitude North Pacific SST anomalies can be represented as a first-order autoregression process (the two-parameter model), i.e. as the response of a system with negative linear feedback to white atmospheric forcing. The average feedback parameter, λ, was found to be about 1 yr^{-1}, or equivalently, the SST anomaly e-folding decay time was $(2\pi)^{-1}$ yr.

5. Acknowledgements

6. Appendix

The test for the validity of each model was determined by defining the probability distribution of ε from (7) for a perfect fit with noise. Since the distribution could be assumed to be Gaussian, it is defined by the first and second moments. In this appendix, these moments are determined.

To begin, let $\bar{E}_j$ be the true spectrum and $\bar{a}_k$ the true fitted kth parameter such that:

$$\bar{E}_j = \hat{E}_j(\bar{a}_k), \tag{A.1}$$

where $E_j \equiv E(f_j)$ and where $k = 1, 2, \ldots, q$. The measured spectrum, E_j, differs from $\bar{E}_j$ by the errors, δE_j:

$$E_j = \bar{E}_j + \delta E_j, \tag{A.2}$$

which results in fitted errors, δa_k, in $\bar{a}_k$ such that the actual fitted parameter, a_k, is:

$$a_k = \bar{a}_k + \delta a_k,$$

and the fitted spectrum is:

$$\hat{E}_j(a_k) = \hat{E}_j(\bar{a}_k) + \delta E_j, \tag{A.3}$$

where

$$\delta E_j(a_k) = \sum_{k=1}^{q} \frac{\partial \hat{E}_j}{\partial a_k} \delta a_k.$$

The next step is to express ε in terms of these definitions by first rewriting (7) as:

$$\varepsilon = \sum_{j=0}^{p-1} [\ln E_j - \ln \hat{E}_j(a_k)]^2. \tag{A.4}$$

With the elimination of E_j and $\hat{E}_j$ by (A.2) and (A.3), and with the use of (A.1), (A.4) reduces to the first-order expression:

$$\varepsilon = \sum_{j=0}^{p-1} \left(\frac{\delta E_j}{\bar{E}_j} - \frac{1}{\hat{E}_j} \sum_{k=1}^{q} \frac{\delta \hat{E}_j}{\partial a_k} \delta a_k \right)^2. \tag{A.5}$$

To now find δa_k in terms of δE_j, (A.4) is minimized to yield:

$$0 = \frac{\partial \varepsilon}{\partial a_k} = \sum_{j=0}^{p-1} 2 (\ln E_j - \ln \hat{E}_j) \frac{1}{\hat{E}_j} \frac{\partial \hat{E}_j}{\partial a_k}, \tag{A.6}$$

for each k. Equations (A.1)–(A.3) permit (A.6) to be reduced to the first-order expression:

$$0 = \sum_{j=0}^{p-1} \left(\delta E_j - \sum_{l=1}^{q} \frac{\partial \hat{E}_j}{\partial a_l} \delta a_l \right) \frac{1}{\hat{E}_j^2} \frac{\partial \hat{E}_j}{\partial a_k}. \tag{A.7}$$

With the definition of:

$$m_{kl} = \sum_{j=0}^{p-1} \frac{1}{\hat{E}_j^2} \frac{\partial \hat{E}_j}{\partial a_k} \cdot \frac{\partial \hat{E}_j}{\partial a_l},$$

as an element of the matrix, M, (A.7) gives the desired result as:

$$\delta a_l = \sum_{j=0}^{p-1} \sum_{k=1}^{q} m_{lk}^{-1} \frac{1}{\hat{E}_j^2} \frac{\partial \hat{E}_j}{\partial a_k} \delta E_j, \tag{A.8}$$

where m_{lk}^{-1} is an element of the inverse of M.

The last intermediate step in finding the moments of the distribution of ε, is to determine the expectation values: $\langle \delta E_j \rangle$ and $\langle \delta E_j^2 \rangle$. Since $v E_j / \bar{E}_j$ is distributed as a χ_v^2-distribution (cf. Jenkins and

Watts, 1968, p. 254) with v degrees of freedom, and a mean and a variance of v and $2v$, respectively, then with the use of (A.2), the expectation values are:

$$\langle \delta E_j \rangle = 0, \tag{A.9}$$

and

$$\frac{\langle \delta E_j^2 \rangle}{\hat{E}_j^2} = \frac{2}{v}. \tag{A.10}$$

To now determine the mean of the distribution of ε, it is necessary to eliminate δa_k in (A.5) with the aid of (A.8) which yields:

$$\varepsilon = \sum_{i=0}^{p-1} \sum_{j=0}^{p-1} R_{ij} \delta E_i \delta E_j, \tag{A.11}$$

where:

$$R_{ij} = \frac{\delta_{ij}}{\hat{E}_j^2} - \frac{1}{\hat{E}_i^2 \hat{E}_j^2} \sum_{k=1}^{q} \sum_{l=1}^{q} m_{lk}^{-1} \frac{\partial \hat{E}_i}{\partial a_l} \frac{\partial \hat{E}_j}{\partial a_k}, \tag{A.12}$$

and δ_{ij} is the Kroneker delta. The expectation value of (A.11) can now be found to be:

$$\langle \varepsilon \rangle = \sum_{j=0}^{p-1} R_{jj} \langle \delta E_j^2 \rangle, \tag{A.13}$$

since $\langle \delta E_i \delta E_j \rangle = 0$ when $j \neq i$.
With the use of (A.10) and (A.12), this finally yields the desired mean:

$$\langle \varepsilon \rangle = \frac{2}{v} (p - q). \tag{A.14}$$

To find the variance, (A.11) is first squared and then the expectation value is taken to give:

$$\langle \varepsilon^2 \rangle = \sum_{i=0}^{p-1} \sum_{j=0}^{p-1} \sum_{k=0}^{p-1} \sum_{l=0}^{p-1} R_{ij} R_{kl} \langle \delta E_i \delta E_j \delta E_k \delta E_l \rangle. \tag{A.15}$$

Since (A.15) was assumed to be Gaussian, then:

$$\langle \delta E_i \delta E_j \delta E_k \delta E_l \rangle \cong \langle \delta E_i \delta E_j \rangle \langle \delta E_k \delta E_l \rangle$$
$$+ \langle \delta E_i \delta E_k \rangle \langle E_j E_l \rangle + \langle \delta E_i \delta_l \rangle \langle \delta E_j \delta E_k \rangle,$$

(cf. Bendat and Piersol, 1966, p. 64) where $\langle \delta E_j \rangle = 0$ by (A.9). Thus (A.15) reduces to:

$$\langle \varepsilon^2 \rangle = \sum_{i=0}^{p-1} \sum_{j=0}^{p-1} (R_{ii} R_{jj} + 2R_{ij}^2) \langle \delta E_i^2 \rangle \langle \delta E_j^2 \rangle. \tag{A.16}$$

The variance can now be expressed as:

$$\langle (\varepsilon - \langle \varepsilon \rangle)^2 \rangle = \langle \varepsilon^2 \rangle - \langle \varepsilon \rangle^2$$
$$= 2 \sum_{i=0}^{p-1} \sum_{j=0}^{p-1} R_{ij}^2 \langle \delta E_i \rangle \langle \delta E_j \rangle, \tag{A.17}$$

by (A.13) and (A.16). A final application of (A.10) and (A.12) permits (A.17) to be reduced to the desired expression for the variance:

$$\langle (\varepsilon - \langle \varepsilon \rangle)^2 \rangle = \frac{8}{v^2} (p - q). \tag{A.18}$$

The probability distribution of ε is now defined by the mean (A.14) and the variance (A.18).

REFERENCES

Bendat, J. S. and Piersol, A. G. 1966. *Measurement and analysis of random data.* New York: John Wiley and Sons.

Copson, E. T. 1960. *An introduction to the theory of functions of a complex variable.* Oxford, Univ. Press.

Davis, R. E. 1976. Predictability of sea surface temperature and sea level pressure over the North Pacific Ocean. *J. Phys. Ocean.* 6, 249–266.

Frankignoul, C. and Hasselmann, K. 1977. Stochastic climate models, Part 2. Application to sea surface temperature anomalies and thermocline variability. *Tellus 29*, 289–305.

Hasselmann, K. 1976. Stochastic climate models, Part 1. Theory. *Tellus 28*, 473–485.

Jenkins, G. M. and Watts, D. G. 1968. *Spectral analysis and its applications.* San Francisco: Holden-Day.

Wunsch, C. 1972. Bermuda sea level in relation to tides, weather, and baroclinic fluctuations. *Rev. Geophys. Space Phys. 10*, 1–49.

АНОМАЛИИ ТЕМПЕРАТУРЫ ПОВЕРХНОСТИ В СЕВЕРНОЙ ЧАСТИ ТИХОГО ОКЕАНА

Аномалии температуры поверхности в средних широтах северной части Тихого океана сравниваются с результатами предсказаний авторегрессионной модели первого порядка, в которой аномалии вызываются локальным белым шумом атмосферы. Результаты показывают, что модель может объяснить спектр мощности аномалий для чуть выше 50% исследуемых областей, главным образом, в центральных областях Тихого океана, но не работает, что неудивительно, в областях резких перемен или океанических фронтов.